Check for updates



www.chemeurj.org

Toward Lung Ventilation Imaging Using Hyperpolarized Diethyl Ether Gas Contrast Agent

Nuwandi M. Ariyasingha,^[a] Md Raduanul H. Chowdhury,^[a] Anna Samoilenko,^[a] Oleg G. Salnikov,^[b] Nikita V. Chukanov,^[b] Larisa M. Kovtunova,^[b, c] Valerii I. Bukhtiyarov,^[c] Zhongjie Shi,^[a] Kehuan Luo,^[a] Sidhartha Tan,^[a] Igor V. Koptyug,^[b] Boyd M. Goodson,^[d] and Eduard Y. Chekmenev*^[a]

Hyperpolarized ¹²⁹Xe gas was FDA-approved as an inhalable contrast agent for magnetic resonance imaging of a wide range of pulmonary diseases in December 2022. Despite the remarkable success in clinical research settings, the widespread clinical translation of HP ¹²⁹Xe gas faces two critical challenges: the high cost of the relatively low-throughput hyperpolarization equipment and the lack of ¹²⁹Xe imaging capability on clinical MRI scanners, which have narrow-bandwidth electronics designed only for proton (¹H) imaging. To solve this translational grand challenge of gaseous hyperpolarized MRI contrast agents, here we demonstrate the utility of batch-mode production of

proton-hyperpolarized diethyl ether gas via heterogeneous pairwise addition of parahydrogen to ethyl vinyl ether. An approximately 0.1-liter bolus of hyperpolarized diethyl ether gas was produced in 1 second and injected in excised rabbit lungs. Lung ventilation imaging was performed using subsecond 2D MRI with up to 2×2 mm² in-plane resolution using a clinical 0.35 T MRI scanner without any modifications. This feasibility demonstration paves the way for the use of inhalable diethyl ether as a gaseous contrast agent for pulmonary MRI applications using any clinical MRI scanner.

Introduction

Functional lung imaging by any technique is notoriously challenging because the lungs are comprised mostly of air-filled alveoli. Non-radioactive natural-abundance Xe gas has been used as a contrast agent with CT but has resulted in low-contrast ventilation images – reducing enthusiasm in this approach. Radioactive single-photon emission computed tomography (SPECT) with Table has been employed for clinical imaging, but it is a 2D projection technique with relatively poor spatial resolution and the disadvantage of exposing the patient to ionizing radiation.

[a] Dr. N. M. Ariyasingha, M. R. H. Chowdhury, Dr. A. Samoilenko, Prof. Z. Shi, Dr. K. Luo, Prof. S. Tan, Prof. E. Y. Chekmenev

Department of Chemistry, Karmanos Cancer Institute (KCI), Department of Pediatrics

Wayne State University Detroit, MI-48202 (USA)

E-mail: chekmenevlab@gmail.com

- [b] Dr. O. G. Salnikov, Dr. N. V. Chukanov, Dr. L. M. Kovtunova, Prof. I. V. Koptyug International Tomography Center SB RAS 3 A Institutskaya Street, Novosibirsk, 630090 (Russia)
- [c] Dr. L. M. Kovtunova, Prof. V. I. Bukhtiyarov Boreskov Institute of Catalysis SB RAS 5 Acad. Lavrentiev Pr, Novosibirsk, 630090 (Russia)
- [d] Prof. B. M. Goodson School of Chemical and Biomolecular Sciences Southern Illinois University Carbondale, IL-62901 (USA)
- Supporting information for this article is available on the WWW under https://doi.org/10.1002/chem.202304071

Conventional proton (1 H) MRI of the lungs is challenging due to the normally low proton density in lung tissue. $^{[3]}$ 1 H MRI is further complicated by the air-tissue interfaces present in alveoli, which produce inhomogeneous magnetic environments that result in short T_2^* relaxation times that decrease image quality. $^{[4,5]}$ Cardiac and respiratory motion further result in imaging quality degradation, leading to dark images of lung void spaces lacking structural detail. Despite advances in imaging techniques such as ultra-short echo time imaging, $^{[6-8]}$ H MRI remains at a distinct disadvantage due to its inability to image lung air spaces.

Noble gas MRI contrast agents such as 129Xe solve this problem - when inhaled, they permit direct visualization of the lung airspaces. [9-13] Provided that 129Xe is hyperpolarized (HP) prior to inhalation, the detection sensitivity is enhanced by 4 orders of magnitude over the corresponding signal at thermal equilibrium, enabling the imaging of low-density gas atoms in pulmonary void spaces. HP gas follows the same pathway as air; HP ¹²⁹Xe also spreads across the alveolocapillary membrane, allowing the calculation of gas exchange parameters including alveolar surface area, septal thickness, and vascular transit time.[14-16] Furthermore, noble gas atoms are not present in the human body; therefore, ¹²⁹Xe MRI yields no background signals - making the resulting MR images easier to interpret.[14-16] HP ¹²⁹Xe contrast agent has shown great utility for pulmonary imaging. Not surprisingly, in December 2022, FDA made a landmark decision to approve the clinical use of hyperpolarized ¹²⁹Xe inhalable gas contrast agent for pulmonary imaging of virtually any lung disease. A wide range of lung imaging applications have been demonstrated^[14,17-20] including functional pulmonary imaging of COVID-19 patients.[16,21-25]

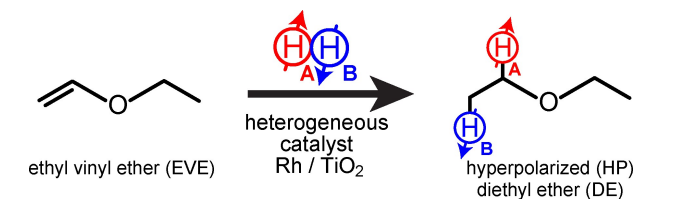
Chemistry Europe European Chemical Societies Publishing

Although modern ¹²⁹Xe hyperpolarizers can produce highly polarized ¹²⁹Xe contrast agent, disadvantages of the technology include: (i) 129Xe hyperpolarizers are bulky and complex devices (due to laser technology limitations) that can be challenging to site and operate.[14,15] Moreover, (ii) these devices often have high cost (~\$0.5 M) and low production throughput (0.5-1 h to produce a human dose) - thereby restricting access to the HP ¹²⁹Xe. [15] Furthermore, (iii) conventional clinical MRI scanners detect only protons, and therefore cannot image ¹²⁹Xe (although in principle clinical MRI scanners can be upgraded to gain the multi-nuclear capability required to perform ¹²⁹Xe MRI, such upgrades are costly (up to \$0.5 M), restricted to select vendor scanner platforms, and not streamlined). These technical challenges have significantly hampered the widespread clinical adaptation of this technology: in a nutshell, such a complex and extensive investment in technology, operating personnel, and infrastructure may be difficult to justify for most clinical radiology programs – both today and in the near future.

Alternative technologies of HP gas production have recently emerged. [26-29] One new technology relies on the production of cheap proton-hyperpolarized hydrocarbon gas using parahydrogen (p-H₂) as a source of hyperpolarization.^[30] Since the produced HP nucleus is proton, such agents can be readily imaged using conventional MRI scanners, [31] thereby potentially mitigating all of the above limitations of the HP 129Xe.[32]

In this work, we show the utility of production of HP diethyl ether (DE) gas and its use for biomedical imaging using a clinical scanner. DE was the first commercialized gaseous anesthetic introduced in 1846. The use of DE anesthetic was phased out in the US and Europe due to flammability issues, although DE remains on the approved list of medical compounds in many other countries.[33] To summarize, our rationale for choosing diethyl ether as an inhalable carrier of hyperpolarization relates to the known low toxicity of DE and the precursor employed for the process of hyperpolarization (ethyl vinyl ether a.k.a. vinamar, which has also been employed as an inhalable anesthetic^[34]).

Heterogeneous parahydrogen-induced polarization (HET PHIP) was employed for production of HP DE gas, where pairwise p-H₂ addition to ethyl vinyl ether (EVE) is performed, Scheme 1. The hydrogenation reaction that breaks the symmetry of p-H₂ nascent protons^[35,36] was performed at the Earth's magnetic field (i.e. within the ALTADENA regime[37]), with the gas subsequently flowing to the high field of an NMR magnet. We have substantially modified the hyperpolarization procedure designed previously for small-scale NMR studies.[38,39] Briefly, liquid ethyl vinyl ether (8 mL) was placed in a 0.7-liter



Scheme 1. Schematic of pairwise p-H₂ addition to ethyl vinyl ether to produce HP DE gas.

aluminum tank equipped with a brass pressure regulator. The tank was then filled with ~4.5 bar p-H₂ gas (~95-98% parastate^[40]). Next, the mixing tank was placed in the oven for 15 min to equilibrate its temperature to 84 °C. Next, the heated tank was removed from the oven (now indicating a gain of pressure by ~2 bar due to EVE evaporation into the gas phase, so the molar ratio of EVE to p-H₂ was estimated to be 1:2) and connected to a reactor made from 1/4" copper tubing and filled with 8 g of copper beads (40-60 mesh size) and 0.2 g of Rh/TiO₂ catalyst (0.9 wt.% Rh content^[41]) via 1/8"-outer-diameter (OD) Teflon tubing. The reactor temperature was > 100 °C (achieved by applying heat using a heat gun or passing a mixture of unsaturated precursor with p-H2 through the reactor prior to MRI scan (the exothermic reaction heats the reactor)). Finally, the tank valve was opened to direct the flow of the p-H₂ / EVE mixture through the reactor, with an estimated flow rate of 8 standard liters per minute of HP gas mixture exiting the reactor (Figure 1a). The exiting HP gas was directed into the excised rabbit lungs (connected to the gas line via trachea) for ventilation MR imaging using a 0.35 T MRI scanner (Figure 1b) or to a benchtop 1.4 T NMR instrument for spectroscopic characterization (Figure 2a-b). All excised rabbit lungs were acquired from unrelated IACUC-approved studies at Wayne State University (animal protocol number is IACUC-23-01-5364; the lungs were excised from the carcasses of the animals euthanized under this animal protocol after the completion of those studies). Approximately 0.15 standard liters of HP DE gas mixture (consisting of HP DE and excess p-H₂) was produced during 1 s. Following the injection of the HP gas, the exiting valve was closed to prevent the back flow of the gas, Figures 1a and 2a.

The imaging sequence of the clinical 0.35 T MRI scanner comprised 16 repeated scans (each 0.94 s), and the first scan was started before the hyperpolarization procedure. The HP DE gas injection occurred after the completion of scan #4 (Figure 1c-1d). The scan #5 revealed a clear presence of HP DE gas in the inflated lungs in axial (Figure 1c) and coronal image (Figure 1d). The proton signal for residual lung tissue is clearly seen in all MR images, and background subtraction was performed in order to remove that intensity - indeed, the images on the right in Figure 1c and Figure 1d reveal the ventilation of gas air space in the lungs (subtracted images for axial and coronal projections are obtained by taking the difference between the inflated lungs with HP DE gas signal and the signal obtained after the inflation image was recorded, Figure 1). The HP DE gas injection procedure was reproducible: indeed, Figure S1 reveals essentially the same coronal visualization with high signal-to-noise ratio (SNR) of 44 versus 46 in Figure 1d. Prompted by the high SNR seen in Figure 1, higherresolution axial and coronal scans were performed (Figure S3) with otherwise-identical parameters, except for a reduced field of view (FOV; 256×256 mm² to 128×128 mm²). These images revealed overall the same features with a smaller pixel size: 2×2 mm² versus 4×4 mm² shown in Figure 1, at the expense of substantially reduced SNR (23 and 14 for axial and coronal projections, respectively, SI).

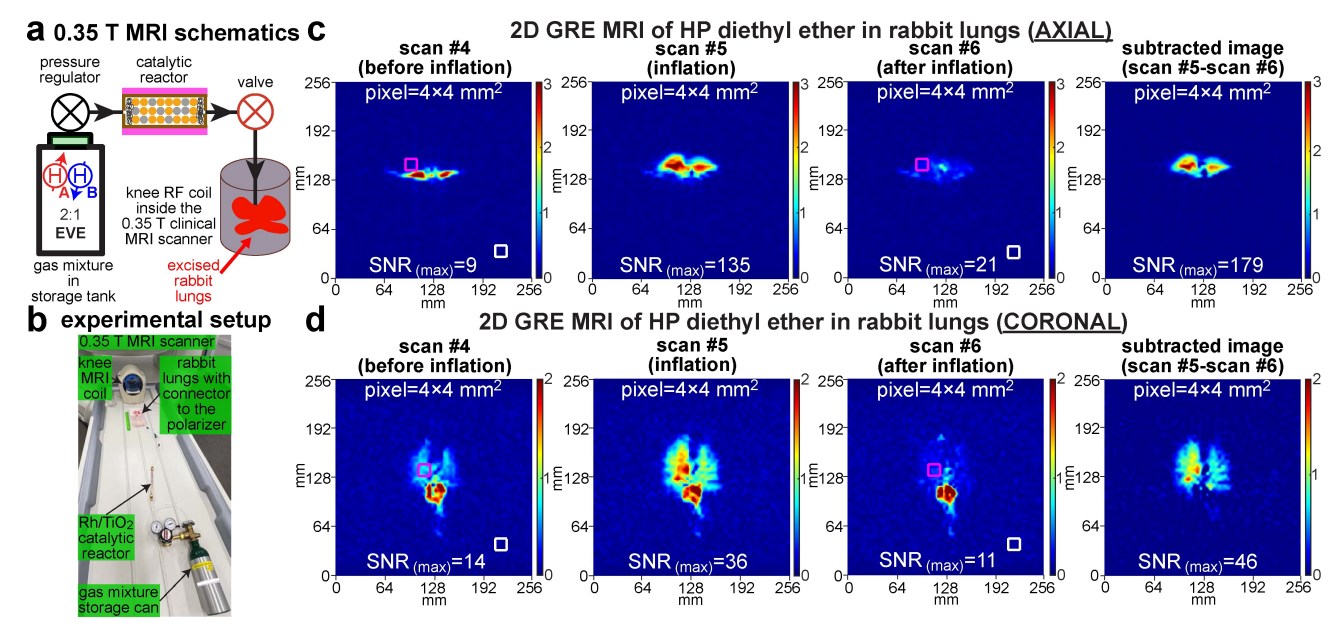


Figure 1. Sub-second 0.35 T 2D MRI of HP DE gas injected in excised rabbit lungs. a) Schematic of experimental setup. b) Annotated photograph of the hyperpolarization equipment and the excised rabbit lungs before placing it inside the knee coil of an open MRI scanner. c) Time series (with 0.94-s temporal resolution) of 2D GRE images (axial projection) recorded from excised rabbit lungs with HP DE gas injection performed, showing the scans before inflation (#4), inflated lungs with HP DE (#5), and after inflation (#6). Note the right image shows background signal subtraction of the "after inflation" image from the "inflation" image. d) Corresponding time series in coronal projection (note the residual background signal intensity seen inside and around the pink box in the image shown in scan #4 due to MRI signal from thermally polarized tissues of collapsed excised lung tissues). All images were acquired with a 256×256 mm² field of view (FOV), slice thickness of 50 mm, 30° slice-selective excitation pulse, 64×64 imaging matrix, and post-processing image interpolation to 256×256 pixels; the SNR_(MAX) was calculated for all displayed images by taking maximum of specific 3×3-pixel matrixes in the signal and dividing it by root mean square (RMS) noise obtained from a similar 3×3-pixel regions marked as pink and white boxes, respectively (see SI for more details).

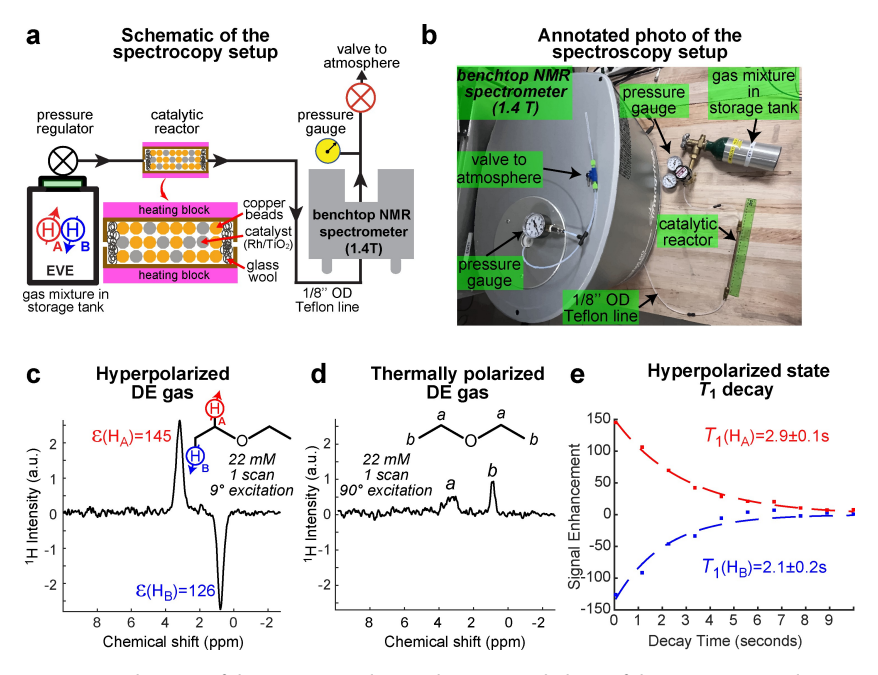


Figure 2. HP DE spectroscopy at 1.4 T. a) Schematic of the experimental setup. b) Annotated photo of the setup; a 30-cm-long green ruler is shown for scale. c) 1 H NMR spectrum of stopped-flow HP DE gas with evaluated signal enhancements of H_{A} and H_{B} resonances. d) The corresponding spectrum of thermally polarized DE gas obtained after hyperpolarization followed by signal decay back to thermal equilibrium at 1.4 T. e) Mono-exponential T_{1} decay of H_{A} and H_{B} resonances of stopped HP DE gas at 1 atm total pressure (the first data point on this curve was obtained by integration of the NMR resonances shown in display c).

The experimental setup employed in the MRI studies was also used for NMR spectroscopy performed on a 1.4 T benchtop NMR spectrometer. In these studies, the 1/8"-OD (1/16"-inner

diameter (ID)) Teflon tubing that contains HP DE gas was placed directly inside the sensing region of NMR spectrometer, allowing for convenient access to HP DE and its spectroscopic

Chemistry Europe

European Chemical Societies Publishing

characterization, Figures 2a, 2b. An NMR spectrum of stopped HP gas (Figure 2c) revealed two HP resonances, corresponding to methylene (H_A) and methyl (H_B) spectral lines with signal enhancements (£) of 145 and 126 respectively at 1.4 T (obtained by signal referencing to thermally polarized spectrum of the same gas, Figure 2d). Quantification of thermally polarized NMR signal revealed the DE concentration of ~22 mM in the gas phase, *i.e.*, ~0.5 bar (the rest was likely unreacted H₂ gas) and near 100% chemical conversion of EVE to DE (SI). The monoexponential decay constant (T_1) of the HP state of the gas at 1.4 T was 2.9 ± 0.1 s and 2.1 ± 0.2 s for H_A and H_B respectively (at clinically relevant total pressure of 1 bar; Figure 2e).

The key limitations of HP DE gas are the relatively short lifetime of HP state - therefore requiring on-site production of HP gas in the proximity of the MRI detectors and fast imaging (both of which are demonstrated here), and the flammability. The DE flammability can be mitigated in three ways. First, a small quantity of HP gas is employed compared to a much larger-scale utilization for anesthetic use to reduce the sheer quantity. Second, exhaled DE gas can be potentially captured using activated-carbon-based filters commonly employed in the workflow of modern gas-based anesthesia. Third, fluorinated EVE derivatives (e.g., trifluoroethyl vinyl ether, a.k.a. fluroxene^[34]) can be potentially employed as a precursor for p-H₂-based production of fluorinated DE derivatives that are known to have substantially reduced flammability.[42] Furthermore, given the short lifetime of the HP state for such gases, a scaled up production (by several fold) may be required for utilization of HP DE in large animals and ultimately in human experimentations - the subject of ongoing work in our partnering laboratories. However, these limitations are arguably outweighed by the key advantages of the presented approach of lung ventilation imaging using HP DE gas, which include: the ultra-low cost of contrast agent production; the simple experimental setup; and the high-speed, essentially on-demand production of the contrast agent that is broadly compatible with clinical MRI scanners that are widely available in hospitals and clinics.

It should be noted that in the presented here pilot HP MRI studies, a 2:1 EVE:p-H₂ precursor gas mixture was employed (Figure 1a). While dihydrogen gas in non-toxic, it is flammable, and future optimization studies should address this translational shortcoming: one potential solution is to employ a 1:1 mixture that in principle should yield HP gas without residual p-H₂ – indeed, example of such approach has been presented for HP propane production from propene and p-H₂.^[32] However, one should be reminded that an inert carrier gas may be required in such mixtures to prevent DE gas condensation due to DE boiling point of 34.6 °C.

The reader should also be reminded of the relatively low toxicity of diethyl ether gas anesthesia, which is typically induced in humans by DE air concentration of 100,000 ppm to 150,000 ppm. The anesthesia is typically maintained at 50,000 ppm DE levels for up to several hours. We envision that in the future, HP DE gas can be potentially administered either as a single HP gas bolus of up to 0.5 liters of DE (resulting in \leq 100,000 ppm in-lung concentration after inhalation and

dilution inside the lungs) or continuously for several minutes (in a manner similar to that of its anesthetic use (*i.e.*, at 50,000 ppm or lower concentration)). Both approaches are anticipated to be safe because they would expose the patients to similar or lower acute concentration and dose of DE.

In summary, we have demonstrated that HP DE gas produced by heterogeneous PHIP can be employed for ventilation imaging of excised rabbit lungs^[43–45] using a clinical MRI scanner without any modification of its hardware or software. The catalyst-free contrast agent gas was produced in approximately one second and expanded into excised rabbit lungs to produce ventilation images with pixel size as small as 2×2 mm² on a 0.35 T MRI scanner equipped with a knee MRI coil. These pilot feasibility studies bode well for future biomedical translation of HP DE gas as a contrast agent for pulmonary MRI applications, hopefully giving new life to a compound that served to improve human health for nearly two centuries.

Acknowledgements

This work was supported by NIH R21HL154032, 1F32HL160108, R01NS114972, R01NS117146, and R01NS130258. O.G.S. and N.V.C. thank the Russian Science Foundation (grant 21-73-10105) for the support of spectroscopic studies of HP DE.

Conflict of Interests

BMG and EYC has a stake of ownership in XEUS Technologies LTD. EYC has a stake of ownership in Vizma Life Sciences LLC.

Data Availability Statement

The data that support the findings of this study are available from the corresponding author upon reasonable request.

Keywords: diethyl ether \cdot parahydrogen \cdot hyperpolarization \cdot PHIP \cdot lung MRI \cdot heterogeneous catalysis

- [1] E. J. Chae, J. B. Seo, Y. S. Cho, Invest. Radiol. 2010, 45, 354.
- [2] W.-J. Shih, G. L. Shih, P. P. Milan, *RadioGraphics* **2010**, *30*, 958–959.
- [3] A. E. Campbell-Washburn, A. A. Malayeri, E. C. Jones, J. Moss, K. P. Fennelly, K. N. Olivier, M. Y. Chen, *Radiology: Cardiothoracic Imaging* 2021, 3, e200611.
- [4] H. Hatabu, D. Alsop, J. Listerud, M. Bonnet, W. B. Gefter, Eur. J. Radiol. 1999, 29, 245–252.
- [5] K. W. Stock, Q. Chen, H. Hatabu, R. R. Edelman, Magn. Reson. Imaging 1999, 17, 997–1000.
- [6] N. L. Muller, J. R. Mayo, C. V. Zwirewich, Am. J. Roentgenol. 1992, 158, 1205–1209.
- [7] J. R. Mayo, A. Mackay, N. L. Muller, Am. J. Roentgenol. 1992, 159, 951–956.
- [8] Y. Ohno, H. Koyama, T. Yoshikawa, K. Matsumoto, M. Takahashi, M. VanCauteren, K. Sugimura, Am. J. Roentgenol. 2011, 197, W279–W258.
- [9] M. Salerno, T. A. Altes, J. P. Mugler, M. Nakatsu, H. Hatabu, E. E. de Lange, Eur. J. Radiol. 2001, 40, 33–44.

Chemistry Europe

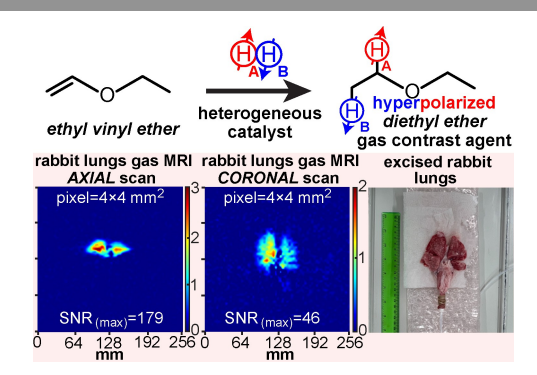
European Chemical Societies Publishing

- [10] H. E. Moller, X. J. Chen, B. Saam, K. D. Hagspiel, G. A. Johnson, T. A. Altes, E. E. de Lange, H.-U. Kauczor, *Magn. Reson. Med.* 2002, 47, 1029–1051.
- [11] E. J. van Beek, J. M. Wild, H. U. Kauczor, W. Schreiber, J. P. Mugler, E. E. de Lange, J. Magn. Reson. Imaging 2004, 20, 540–554.
- [12] S. Matsuoka, S. Patz, M. S. Albert, Y. Sun, R. R. Rizi, W. B. Gefter, H. Hatabu, J. Thorac. Imaging 2009, 24, 181–188.
- [13] S. Fain, M. L. Schiebler, D. G. McCormack, G. Parraga, J. Magn. Reson. Imaging 2010, 1398–1408.
- [14] J. P. Mugler, T. A. Altes, J. Magn. Reson. Imaging 2013, 37, 313-331.
- [15] A. S. Khan, R. L. Harvey, J. R. Birchall, R. K. Irwin, P. Nikolaou, G. Schrank, K. Emami, A. Dummer, M. J. Barlow, B. M. Goodson, E. Y. Chekmenev, Angew. Chem. Int. Ed. 2021, 60, 22126–22147.
- [16] L. L. Walkup, J. C. Woods, NMR Biomed. 2014, 27, 1429-1438.
- [17] Y. Ding, L. Yang, Q. Zhou, J. Bi, Y. Li, G. Pi, W. Wei, D. Hu, Q. Rao, H. Li, L. Zhao, A. Liu, D. Du, X. Wang, X. Zhou, G. Han, K. Qing, J. Appl. Clin. Med. Phys. 2022, 23, e13502.
- [18] J. G. Mammarappallil, L. Rankine, J. M. Wild, B. Driehuys, J. Thorac. Imaging 2019, 34, 136–150.
- [19] P. J. Niedbalski, E. A. Bier, Z. Wang, M. M. Willmering, B. Driehuys, Z. I. Cleveland, J. Appl. Physiol. 2020, 129, 218–229.
- [20] R. S. Virgincar, J. C. Nouls, Z. Wang, S. Degan, Y. Qi, X. Xiong, S. Rajagopal, B. Driehuys, Sci. Rep. 2020, 10, 7385.
- [21] H. Li, X. Zhao, Y. Wang, X. Lou, S. Chen, H. Deng, L. Shi, J. Xie, D. Tang, J. Zhao, L.-S. Bouchard, L. Xia, X. Zhou, Sci. Adv. 2021, 7, eabc8180.
- [22] L. L. Walkup, R. P. Thomen, T. G. Akinyi, E. Watters, K. Ruppert, J. P. Clancy, J. C. Woods, Z. I. Cleveland, *Pediatr. Radiol.* 2016, 46, 1651–1662.
- [23] R. P. Thomen, L. L. Walkup, D. J. Roach, Z. I. Cleveland, J. P. Clancy, J. C. Woods, J. Cystic Fibrosis 2017, 16, 275–282.
- [24] D. A. Barskiy, A. M. Coffey, P. Nikolaou, D. M. Mikhaylov, B. M. Goodson, R. T. Branca, G. J. Lu, M. G. Shapiro, V.-V. Telkki, V. V. Zhivonitko, I. V. Koptyug, O. G. Salnikov, K. V. Kovtunov, V. I. Bukhtiyarov, M. S. Rosen, M. J. Barlow, S. Safavi, I. P. Hall, L. Schröder, E. Y. Chekmenev, *Chem. Eur. J.* 2017, 23, 725–751.
- [25] R. L. Eddy, G. Parraga, Eur. Respir. J. 2020, 55, 1901987.
- [26] K. V. Kovtunov, I. V. Koptyug, M. Fekete, S. B. Duckett, T. Theis, B. Joalland, E. Y. Chekmenev, Angew. Chem. Int. Ed. 2020, 59, 17788–17797
- [27] L. S. Bouchard, K. V. Kovtunov, S. R. Burt, M. S. Anwar, I. V. Koptyug, R. Z. Sagdeev, A. Pines, *Angew. Chem. Int. Ed.* 2007, 46, 4064–4068.
- [28] K. V. Kovtunov, D. A. Barskiy, A. M. Coffey, M. L. Truong, O. G. Salnikov, A. K. Khudorozhkov, E. A. Inozemtseva, I. P. Prosvirin, V. I. Bukhtiyarov, K. W. Waddell, E. Y. Chekmenev, I. V. Koptyug, *Chem. Eur. J.* 2014, 20, 11636–11639.
- [29] E. V. Pokochueva, D. B. Burueva, O. G. Salnikov, I. V. Koptyug, ChemPhysChem 2021, 22, 1421–1440.

- [30] I. V. Koptyug, K. V. Kovtunov, S. R. Burt, M. S. Anwar, C. Hilty, S. I. Han, A. Pines, R. Z. Sagdeev, J. Am. Chem. Soc. 2007, 129, 5580–5586.
- [31] O. G. Salnikov, P. Nikolaou, N. M. Ariyasingha, K. V. Kovtunov, I. V. Koptyug, E. Y. Chekmenev, Anal. Chem. 2019, 91, 4741–4746.
- [32] N. M. Ariyasingha, A. Samoilenko, J. R. Birchall, M. R. H. Chowdhury, O. G. Salnikov, L. M. Kovtunova, V. I. Bukhtiyarov, D. C. Zhu, C. Qian, M. Bradley, J. G. Gelovani, I. V. Koptyug, B. M. Goodson, E. Y. Chekmenev, ACS Sens. 2023, 8, 3845–3854.
- [33] C. Y. Chang, E. Goldstein, N. Agarwal, K. G. Swan, *BMC Anesthesiol.* **2015**, *15*, 149–149.
- [34] H. M. Slater, Can. Anaes. J. 1957, 4, 5–12.
- [35] C. R. Bowers, D. P. Weitekamp, Phys. Rev. Lett. 1986, 57, 2645–2648.
- [36] T. C. Eisenschmid, R. U. Kirss, P. P. Deutsch, S. I. Hommeltoft, R. Eisenberg, J. Bargon, R. G. Lawler, A. L. Balch, J. Am. Chem. Soc. 1987, 109, 8089–8091.
- [37] M. G. Pravica, D. P. Weitekamp, Chem. Phys. Lett. 1988, 145, 255-258.
- [38] N. M. Ariyasingha, B. Joalland, H. R. Younes, O. G. Salnikov, N. V. Chukanov, K. V. Kovtunov, L. M. Kovtunova, V. I. Bukhtiyarov, I. V. Koptyug, J. G. Gelovani, E. Y. Chekmenev, Chem. Eur. J. 2020, 26, 13621–13626
- [39] O. G. Salnikov, A. Svyatova, L. M. Kovtunova, N. V. Chukanov, V. I. Bukhtiyarov, K. V. Kovtunov, E. Y. Chekmenev, I. V. Koptyug, *Chem. Eur. J.* 2021, 27, 1316–1322.
- [40] S. Nantogma, B. Joalland, K. Wilkens, E. Y. Chekmenev, Anal. Chem. 2021, 93, 3594–3601.
- [41] D. A. Barskiy, K. V. Kovtunov, E. Y. Gerasimov, M. A. Phipps, O. G. Salnikov, A. M. Coffey, L. M. Kovtunova, I. P. Prosvirin, V. I. Bukhtiyarov, I. V. Koptyug, E. Y. Chekmenev, J. Phys. Chem. C 2017, 121, 10038–10046.
- [42] B. Joalland, N. M. Ariyasingha, H. R. Younes, S. Nantogma, O. G. Salnikov, N. V. Chukanov, K. V. Kovtunov, I. V. Koptyug, J. G. Gelovani, E. Y. Chekmenev, Chem. Eur. J. 2021, 27, 2774–2781.
- [43] Z. Shi, K. Luo, S. Jani, M. February, N. Fernandes, N. Venkatesh, N. Sharif, S. Tan, J. Neurosci. Res. 2022, 100, 2138–2153.
- [44] J. Vasquez-Vivar, Z. Shi, J.-W. Jeong, K. Luo, A. Sharma, K. Thirugnanam, S. Tan, Redox Biol. 2020, 29, 101407.
- [45] J. Vasquez-Vivar, Z. Shi, K. Luo, K. Thirugnanam, S. Tan, *Redox Biol.* 2017, 13, 594–599.

Manuscript received: December 13, 2023
Accepted manuscript online: February 21, 2024
Version of record online:

RESEARCH ARTICLE



Hyperpolarized diethyl ether gas was produced via heterogeneous pairwise parahydrogen addition to ethyl vinyl ether (a.k.a. vinamar) anesthetic gas and employed for a pilot feasibility demonstration to record sub-second 2D ventilation MRI of excised rabbit lungs on a clinical 0.35 T MRI scanner without any modifications to the scanner's hardware or software.

Dr. N. M. Ariyasingha, M. R. H. Chowdhury, Dr. A. Samoilenko, Dr. O. G. Salnikov, Dr. N. V. Chukanov, Dr. L. M. Kovtunova, Prof. V. I. Bukhtiyarov, Prof. Z. Shi, Dr. K. Luo, Prof. S. Tan, Prof. I. V. Koptyug, Prof. B. M. Goodson, Prof. E. Y. Chekmenev*

1 – 6

Toward Lung Ventilation Imaging
Using Hyperpolarized Diethyl Ether
Gas Contrast Agent